Neurobiology of Aging 83 (2019) 86–94

Contents lists available at ScienceDirect

Neurobiology of Aging

journal homepage: www.elsevier.com/locate/neuaging

Regional brain atrophy predicts time to conversion to Alzheimer's disease, dependent on baseline volume

Hossein Tabatabaei-Jafari [a,*], Marnie E. Shaw [b], Erin Walsh [a], Nicolas Cherbuin [a], For the Alzheimer's Disease Neuroimaging Initiative (ADNI)[1]

[a] Centre for Research on Ageing, Health and Wellbeing, The Australian National University, Canberra, Australia
[b] Research School of Electrical, Energy and Materials Engineering, College of Engineering and Computer Science, The Australian National University, Canberra, Australia

ARTICLE INFO

Article history:
Received 15 January 2019
Received in revised form 29 August 2019
Accepted 31 August 2019
Available online 10 September 2019

Keywords:
Hippocampus
Mild cognitive impairment
Alzheimer's disease
Time to conversion
Interaction
MRI

ABSTRACT

A key question for the design of clinical trials for Alzheimer's disease (AD) is whether the timing of conversion from mild cognitive impairment (MCI) to AD can be predicted. This is also an important question for the clinical management of MCI. This study aims to address this question by exploring the contribution of baseline brain volume and annual volume change, using Cox regression, in predicting the time to conversion. Individuals with MCI, who converted to AD (n = 198), reverted to normal (n = 38), or remained stable (n = 96) for at least five years, were included in this study. The results revealed that the volumes of all the brain areas considered were predictive of the time to conversion from MCI to AD. Annual change in volume was also predictive of the time to conversion but only when initial volumes were above a certain threshold. This is important because it suggests that reduction in atrophy rate, which is the outcome of some clinical trials, is not inevitably associated with delay in conversion from MCI to AD.

1. Introduction

Progressive neurodegeneration is a hallmark of Alzheimer's disease (AD). However, it is also prevalent in normal aging (Fjell et al., 2014). One major difference is that the rate of degeneration in the pathological progression leading to AD is substantially higher than in normal aging. A meta-analysis of longitudinal studies conducted in the last two decades revealed that the shrinkage rate in the prodromal stage of AD—mild cognitive impairment (MCI)—is at least twice that observed in normal aging (Tabatabaei-Jafari et al., 2015). This is seen in the whole brain and even more so in brain areas typically more affected in the first stage of the disease, such as the hippocampus and entorhinal cortex. Moreover, degeneration begins decades before the disorder emerges clinically, sometimes even in early adulthood (Braak and Braak, 1997). These findings underpin the hope that early intervention aimed at decreasing brain shrinkage may stop, or at least slow down, further progression to clinical AD.

Several intervention trials, using nutrient supplements or medication, have been effective in reducing the atrophy rate in total or regional brain volumes in those with MCI (Douaud et al., 2013; Dubois et al., 2015; Kile et al., 2017; Kobe et al., 2016; Prins et al., 2014; Zhang et al., 2017). However, whether these changes can modify the course of AD progression and delay the time to conversion remains an unresolved question. To address such questions, it is necessary to better understand the contribution brain atrophy makes to the course of the disease and particularly to the progression from MCI to AD.

In contrast to studies predicting conversion from MCI to AD, studies that have investigated the time to conversion are limited in number. They generally suggest an association between the pace of neurodegeneration and the time to AD conversion (Falahati et al., 2017; Jack et al., 2005; Liu et al., 2017; Teipel et al., 2015). Most attempts have used spatial patterns of longitudinal volume loss (using machine learning) to successfully predict the time to conversion (Gavidia-Bovadilla et al., 2017; Li et al., 2012; Risacher et al., 2010; Teipel et al., 2015; Thung et al., 2018). Falahati el al. developed a "severity index", based on degeneration in 34 measures of regional cortical thickness and 21 regional subcortical volumes and showed

* Corresponding author at: Centre for Research on Ageing, Health and Wellbeing, Florey Building 54, Mills Road, Australian National University, Acton, Australian Capital Territory, 2601 Australia. Tel: (612) 61259032; fax: (612) 61251558.
E-mail address: hossein.tabatabaei@anu.edu.au (H. Tabatabaei-Jafari).

[1] Data used in preparation of this article were obtained from the Alzheimer's Disease Neuroimaging Initiative (ADNI) database (adni.loni.usc.edu). As such, the investigators within the ADNI contributed to the design and implementation of ADNI and/or provided data but did not participate in analysis or writing of this report. A complete listing of ADNI investigators can be found in the Supplemental file.

0197-4580/$ – see front matter © 2019 Elsevier Inc. All rights reserved.
https://doi.org/10.1016/j.neurobiolaging.2019.08.033

that it was predictive of the time to AD conversion for up to 3 years follow-up. The index showed 95% correct prediction of conversion within the first year and 80% over 3 years (Falahati et al., 2017). Global volume change such as whole brain atrophy and ventricular enlargement, but not regional brain atrophy rates (hippocampal and entorhinal cortex), has also been shown to be predictive of AD conversion but only for a short follow-up and in the context of a relatively small study (Jack et al., 2005). Although these limited numbers of studies are conceptually supportive of the idea that faster degeneration will lead to earlier conversion, the findings are based on a short-term follow-up and the approaches are complex and methodologically difficult to implement at individual level that is a requirement for clinical trials and clinical practice. Simple measures such as regional brain volume and regional atrophy rate investigated in a longer follow-up may be more practical for individual evaluation, especially in a clinical setting or for clinical trials.

Therefore, strong evidence supporting the use of atrophy rate in the prediction of time to conversion from MCI to AD is still lacking. In addition, it is necessary to clarify the extent to which the predictive value of atrophy rate depends on baseline volume. This is needed because the clinical impact of any future degeneration is likely to be highly dependent on prior atrophy and/or brain reserve indexed by the current volume of a region of interest. To address these questions, the present study aimed to investigate the value of global as well as regional baseline volume and atrophy rate and their interaction over long-term follow-ups in predicting conversion from MCI to AD.

2. Methodology

2.1. Study participants

Data used in the preparation of this article were obtained from the Alzheimer's Disease Neuroimaging Initiative (ADNI) database (adni.loni.usc.edu). ADNI was launched in 2003 as a public-private partnership, led by Principal Investigator Michael W. Weiner, MD. The primary goal of ADNI has been to test whether serial magnetic resonance imaging (MRI), positron emission tomography, other biological markers, and clinical and neuropsychological assessment can be combined to measure the progression of MCI and early AD.

All participants of ADNI 1/GO/2, who were diagnosed with MCI at the baseline, remained stable for at least six months, and underwent MRI scanning more than twice, were considered for inclusion. Individuals with MCI who converted to AD (MCIc, n = 198), reverted to cognitively normal (CN; MCIr, n = 38), or remained stable for more than five years (MCIs, n = 96) were included in this study.

Details of the diagnostic criteria can be found at the ADNI web site (http://www.adni-info.org/Scientists/AboutADNI.aspx). Briefly, participants were classified as MCI if they had a Mini–Mental State Examination (MMSE) score greater than 24, a CDR of 0.5, a report of subjective memory concern, an objective memory loss, preserved daily living activity, and did not meet diagnostic criteria for dementia. Participants were classified as AD if they had an MMSE score less than 26, CDR of 0.5 or above, and fulfilled criteria for clinically probable AD according to the Institute of Neurological and Communicative Diseases and Stroke/Alzheimer's Disease and Related Disorders Association. It is also important to note that a Geriatric Depression Scale score of less than 6 was a requirement for participation in the ADNI study (Petersen et al., 2010), so all participants had a Geriatric Depression Scale score of normal range.

2.2. Neuroimaging acquisition and processing

Participants underwent high-resolution MRI brain scans on 1.5 (N = 889) or 3 T (N = 872) scanners from General Electric, Siemens, or Philips (Milwaukee, WI, USA; Germany; the Netherlands, respectively) using a standardized ADNI acquisition protocol for 3D MP-RAGE sequence (Jack et al., 2008). Images which had undergone specific ADNI preprocessing correction steps to standardize images from different sites and platforms were obtained for this study: (1) Grad wrap: a specific correction of image geometry distortion due to nonlinearity, (2) B1 nonuniformity: B1 calibration to correct the image intensity nonuniformity that results when RF transmission is performed with a more uniform body coil while reception is performed with a less-uniform head coil, (3) N3 correction: a histogram peak sharpening algorithm applied after grad wrap and B1 correction. For MCI participants, only images acquired before conversion to AD or reversion to CN were included. The MRI scans of individual participants were acquired on the same scanner with the same parameters throughout the follow-up.

All scans were segmented with FreeSurfer version 5.3 (http://surfer.nmr.mgh.harvard.edu/), processed with the longitudinal pipeline. For each participant, all scans were initially processed by the default workflow. Then an unbiased template (an average template) was created from all time points. The unbiased template was used as a base for registering all the time point scans to reduce the random within-subject variation in the processing procedure of the longitudinal analysis. Finally, all time points were longitudinally processed.

The output-segmented images were visually checked. The criterion was a clear segmentation error as assessed by an experienced neuroscientist. Scans with segmentation errors were reprocessed and would only be excluded if the error could not be corrected. Six scans with error were not correctable and excluded from the study.

2.3. Measurements

Four brain volumes were considered as regions of interest (ROIs) in this study: (1) total whole brain volume (sum of the total gray and white matter), (2) total ventricular volume (sum of the lateral, third, and fourth ventricular volumes), (3) total hippocampal volume (sum of the left and right hippocampus), and (4) total entorhinal cortex volume (sum of the left and right entorhinal cortex). Baseline volume and annual change rate (atrophy rate for the whole brain, hippocampus, and entorhinal cortex and enlargement rate for the ventricles) of each ROI were investigated as the measures of interest for predicting time to conversion from MCI to AD.

The annual change rate for each ROI was computed by the least square linear regression method for each individual separately: brain volume (at each time point) was used as the dependent variable, with age at each time point (centered at 55, the minimum age at the baseline) as the independent variable. The regression coefficient for age was considered as the volume change for each year increase in age in mm^3. The regression coefficient was used to compute the annual change rate in percentage using the formula

$$100 \times (\textit{the regression coefficient for age} / \textit{baseline volume})$$

Because the results from our previous study revealed that the baseline scores on the MMSE, the Alzheimer's Disease Assessment Scale (ADAS cognitive version), the Functional Assessment Questionnaire, and the Rey Auditory Learning Test (immediate memory subtype) were predictive of time to conversion from MCI to AD when also taking into account hippocampal volume (Tabatabaei-Jafari et al., 2019), the annual change rates of these measures were also evaluated to better characterize the participants.

While CSF level of amyloid β 1-42 and total and phosphorylated tau were only available for a subsample of participants (236 for amyloid β, 232 for total tau, and 236 for phosphorylated tau of the

332 participants), they could not be included in analyses but are reported to better characterize the sample investigated.

2.4. Statistical analysis

Statistical analyses were performed using the R statistical software (version 3.3.2). Data were checked for missing values and for univariate and multivariate outliers using Mahalanobis distance. There were no missing values or outliers. Group differences in demographic variables were assessed by *t*-test for continuous variables and chi-square tests for categorical variables. The alpha level was set at < 0.05.

Cox regression analysis (package survival; version 2.40–1) using time to event as time metric was used to investigate the predictive value of brain ROIs for time to conversion from MCI to AD. The event in the model was specified as happened if the individual converted to AD, thus MCIc were coded as 1 and MCIs and MCIr were coded as 0 in the model. For MCIs, the time to event was the time from the baseline to the last scan, whereas in MCIc and MCIr, it was the time from the baseline to diagnosis change (change to AD for MCIc and change to CN for MCIr). One-sided Wald tests were used to test associations because only increase in the risk of conversion to AD was predicted. Baseline volume and annual change rate were considered as predictors of time to conversion and were standardized to reduce the variance inflation factor in the model. Baseline volumes were adjusted for age, sex, field strength, and intracranial volume using the residual method before adopted in the models (Pintzka et al., 2015).

Table 1
Participants characteristic and measurements

Diagnostic group	MCIr	MCIs	MCIc	Significant pair difference ($p < 0.05$)
Sample size	38	96	198	-
Age; year, mean (SD)	69.30 (8.23)	71.65 (7.48)	74.25 (7.16)	MCIc vs. MCIr and MCIs
Age range, year	55–87	57–88	55–89	-
Male sex; N (%)	18 (47.37)	58 (60.42)	121 (61.42)	No difference
Education; year, mean (SD)	16.68 (2.52)	15.88 (3.04)	16.01 (2.78)	No difference
APOE e4; N (%)				
One allele	17 (45)	22 (23)	102 (51.51)	MCIc vs. MCIr and MCIs
Two alleles	1 (3)	6 (6)	32 (16.33)	MCIr vs. MCIs
Number of scan points	11.4 (2.7)	7.7 (2.5)	5.9 (1.8)	MCIc vs. MCIr and MCIs MCIr vs. MCIs
Follow-up, range; day	1082 - 3662	1850 - 3927	343 - 3690	-
Follow-up, mean (SD)	1704 (676)	2381 (686)	1790 (869)	-
Time to diagnosis change, range; day	184–1583	-	357–3714	-
Time to DX change, mean (SD)	762 (411)	-	1041 (603)	-
Brain measures				
Whole brain				
Baseline, mm^3	1,081,597 (35,162)	1,095,415 (38,165)	1,070,628 (42,231)	MCIc vs. MCIs MCIr vs. MCIs
Annual change rate, %/y	−0.15 (1.20)	−0.55 (0.37)	−0.73 (1.26)	MCIc vs. MCIr MCIr vs. MCIs
Ventricles				
Baseline, mm^3	37,782 (14,261)	38,808 (15,115)	44,744 (17,982)	MCIc vs. MCIr and MCIs
Annual change rate, %/y	2.42 (3.94)	3.93 (2.66)	7.62 (5.74)	MCIc vs. MCIr and MCIs MCIr vs. MCIs
Hippocampus				
Baseline, mm^3	7229 (794)	7035 (953)	6127 (912)	MCIc vs. MCIr and MCIs
Annual change rate, %/y	0.13 (3.34)	−1.29 (1.10)	−3.12 (2.86)	MCIc vs. MCIr and MCIs MCIr vs. MCIs
Entorhinal cortex				
Baseline, mm^3	3787 (693)	3645 (644)	3224 (698)	MCIc vs. MCIr and MCIs
Annual change rate, %/y	−0.11 (5.05)	−1.75 (1.56)	−3.62 (5.95)	MCIc vs. MCIr and MCIs
Cognitive/functional measures				
MMSE				
Baseline	28.53 (1.50)	28.22 (1.42)	27.09 (1.78)	MCIc vs. MCIr and MCIs
Annual change, u/y	0.64 (1.94)	−0.15 (0.29)	−0.93 (1.94)	MCIc vs. MCIr and MCIs MCIr vs. MCIs
ADAS cog				
Baseline	10.66 (4.24)	12.08 (4.63)	19.94 (5.81)	MCIc vs. MCIr and MCIs
Annual change, u/y	−1.97 (4.31)	0.24 (0.57)	1.50 (3.98)	MCIc vs. MCIr and MCIs MCIr vs. MCIs
RAVLT immediate				
Baseline	43.55 (10.21)	39.70 (10.96)	29.64 (7.98)	MCIc vs. MCIr and MCIs
Annual change, u/y	−1.44 (7.88)	−0.46 (1.44)	−2.06 (6.14)	MCIc vs. MCIs
FAQ				
Baseline	0.87 (1.73)	1.60 (3.07)	4.61 (4.54)	MCIc vs. MCIr and MCIs
Annual change, u/y	−0.16 (2.35)	0.22 (0.69)	1.61 (3.55)	MCIc vs. MCIr and MCIs
CSF measures (baseline)				
Amyloid β level, pg/mL	211.54 (50.51)	198.23 (48.10)	143.19 (42.85)	MCIc vs. MCIr and MCIs
TAU	60.24 (29.31)	75.21 (49.97)	115.45 (55.86)	MCIc vs. MCIr and MCIs
P-TAU	27.69 (14.45)	32.21 (49.97)	49.61 (26.13)	MCIc vs. MCIr and MCIs

Baseline measures adjusted for age, sex, field strength, and intracranial volume.
Key: MCIc, mild cognitive impairment converted to Alzheimer's disease; MCIs, mild cognitive impairment remained stable for more than five years; MCIr, mild cognitive impairment reverted to cognitively; APOE e4, apolipoprotein E allele 4; MMSE, Mini–Mental State Examination; ADAS cog, Alzheimer's Disease Assessment Scale (cognitive subscale); RAVLT, Rey Auditory Verbal Learning Test; FAQ, functional assessment questionnaire; CSF, cerebrospinal fluid; Aβ, amyloid-beta 1–42; TAU, total tau protein; P-TAU, phosphorylated tau protein.

Univariate models were used to investigate the association between brain measures and time to conversion. Four separate bivariate models, each consisting of standardized baseline volume, standardized annual change rate, and their interaction, were conducted for the whole brain, ventricles, hippocampus, and entorhinal cortex. Hazard ratios with 95% confidence intervals for a 1-SD different in baseline volume and 1-SD change in annual change rate were used to quantify the magnitude of the effect. In the case of significant interaction between baseline volume and annual change rate (as continuous variables), to better conceptualize the interaction, participants were categorized into 3 groups based on their baseline volume (for each brain area separately) and the bivariate analyses were repeated with categorical baseline volume in the model. Categorization was based on the standard deviation (SD, round values): (1) small category: smaller than 1 SD below the mean, (2) medium category: 1 SD below and above the mean, and (3) large category: larger than one SD above the mean. In addition, to better visualize the contribution of baseline volume and annual change rate in predicting conversion from MCI to AD, the density of those converted to AD over time was plotted across different stratified annual change rate for each baseline volume category separately.

3. Results

3.1. Participants' characteristics

Three hundred thirty-two participants (59% male), who were followed up for up to ten years (5.35 ± 2.31 years), were categorized into MCIr, MCIs, and MCIc (Table 1). Individuals with MCIc were about three years older than other individuals with MCI. There was no significant difference in education across the groups, but the proportion of males was somewhat lower in MCIr (47.37%) than in MCIs (60.42%) and MCIc (60.42%). The proportion of individuals carrying the APOE e4 allele was significantly larger in MCIc than others, and more so for those with two e4 alleles (Table 1, Supplementary table 1).

3.2. Baseline brain volumes and annual changes

For all ROIs, baseline volumes and annual change rates were different between MCIc and other MCI types. Differences were most pronounced in the hippocampus, entorhinal cortex, and ventricles and followed the direction MCIr > MCIs > MCIc for volumes, and MCIr < MCIs < MCIc for change rates (Table 1, Supplementary table 1).

Despite significant group differences, the distribution of the brain measures revealed a large overlap across the groups (Supplementary Fig. 1). When considered across the whole sample, there was no significant correlation between baseline volume and annual change rate for the whole brain and the ventricles. A moderate correlation was detected for the hippocampus (r = 0.27), and a smaller correlation for the entorhinal cortex (r = 0.12). However, when computed separately in each group, associations between baseline volume and annual change rate were only significant in MCIs for the hippocampus and entorhinal cortex as well as for the ventricles in MCIc (r = −0.19) (Supplementary table 2).

3.3. Cognitive/functional measures

Similar to brain measures, cognitive/functional measures were significantly different between MCIc and other MCI types. Differences were most pronounced in baseline volumes following the order MCIr <MCIs <MCIc. While annual changes were significantly different between MCIc and other MCI types, differences between MCIr and MCIs did not follow a constant pattern (Table 1, Supplementary table 1).

3.4. CSF measures

The pattern in CSF differences was consistent (in the subsample that data were available) across the groups. Amyloid β was significantly lower in MCIc than MCIs and MCIr, and total tau and phosphorylated tau were significantly greater in MCIc than MCIs and MCIr. These measures were not different between MCIr and MCIs (Table 1, Supplementary table 1).

3.5. Prediction of time to AD conversion

Baseline volume and annual change rate for each brain area significantly predicted time to AD conversion ($Z > 5$, $p < 0.01$) when they were evaluated separately (univariate model). When baseline volume and annual change rate were tested in the same model (bivariate model) both measures remained significantly predictive in all ROIs. In addition, an interaction between annual change rate and baseline volume was detected. It means, in

Table 2
Cox proportional hazard

Diagnostic group	Coef.	SE	HR (95% CI)	Z
Whole brain				
Baseline volume	0.43	0.08	1.53 (1.31–1.79)	**5.344, $p < 0.0001$**
Annual atrophy rate	0.32	0.09	1.38 (1.15–1.65)	**4.024, $p < 0.0001$**
Interaction	0.21	0.07	1.24 (1.08–1.41)	**3.110, $p < 0.01$**
Ventricles				
Baseline volume	0.25	0.07	1.29 (1.14–1.46)	**3.919, $p < 0.0001$**
Annual enlargement rate	0.46	0.06	1.58 (1.41–1.77)	**7.988, $p < 0.0001$**
Interaction	−0.16	0.08	0.85 (0.73–0.99)	**−2.133, $p < 0.05$**
Hippocampus				
Baseline volume	0.63	0.08	1.87 (1.60–2.19)	**7.840, $p < 0.0001$**
Annual atrophy rate	0.66	0.10	1.94 (1.61–2.33)	**7.001, $p < 0.0001$**
Interaction	0.45	0.09	1.56 (1.30–1.88)	**4.755, $p < 0.0001$**
Entorhinal cortex				
Baseline volume	0.44	0.08	1.55 (1.33–1.80)	**5.671, $p < 0.0001$**
Annual atrophy rate	0.56	0.10	1.75 (1.45–2.12)	**5.768, $p < 0.0001$**
Interaction	0.30	0.10	1.35 (1.11–1.64)	**3.061, $p < 0.01$**

All measures have been adjusted for age, field strength, and intracranial volume.
Bolded values represents the significance of $p < 0.05$.
Key: HR, hazard ratio for 1-SD decrease in whole brain, hippocampal volume and entorhinal cortex volume and their annual rates as well as 1-SD increase in ventricular volume and its annual ventricular volume enlargement.

addition to a constant increase in the risk for each 1-SD decrease in ROIs' baseline volume (1-SD increase in ventricular volume) and 1-SD increase in annual volume loss, there was an additional risk for each measure, which was dependent on the other measure (Table 2). To better conceptualize this interactive effect between the 2 measures, analyses were repeated with a categorical baseline volume (small, medium and large) and annual change rate in percent in the model (Table 3). Following are brief reports for each ROI separately.

Because APOE e4 carrier prevalence was significantly higher in MCIc than other MCI types, post hoc analyses were carried out to investigate the effect of APOE e4 on the predictive values of baseline volumes and annual change rates and their interactions. The result showed that APOE e4 genotype had no effect on the predictive values of these measures as well as their interactions.

Fig. 1 demonstrates the distribution of individuals converted from MCI to AD within ten years using Cox analysis to estimate probability in each separate baseline category across stratified annual atrophy rates (enlargement rate for the ventricles). It reveals that at hippocampal baseline volumes less than 5500 mm^3, conversion within 3 years occurs regardless of the atrophy rate. A similar but somewhat weaker pattern was observed for an entorhinal cortex volume smaller than 2800 mm^3, a whole brain volume smaller than 1,040,000 mm^3, and a ventricular volume larger than 55,000 mm^3. By contrast, atrophy rate (enlargement rate for the ventricles) is determinant of probability of conversion over time at medium to large baseline brain volumes (medium to small for the ventricles). It is especially noticeable for the hippocampus with atrophy rate more than the average.

3.5.1. Whole brain

Atrophy rate did not predict time to conversion in whole brain baseline volumes less than 1,040,000 mm^3, whereas it had significant predictive value at higher volumes. Medium to large whole brain volumes were associated with 61% and 72% lower risk of conversion from MCI to AD compared with small volumes. An additional 35% and 43% decrease in the risk of conversion were demonstrated for every 1 percent lower atrophy rate in medium and large volumes.

3.5.2. Ventricles

Enlargement rate did not predict time to conversion in ventricular baseline volumes larger than 55,000 mm^3, whereas it had significant predictive value at small volumes (lower than 28,000 mm^3). Medium to small volumes were, respectively, associated with 48% and 83% lower risk of conversion from MCI to AD compared with large volumes. An additional 14% increase in the risk of conversion was demonstrated for 1 percent greater enlargement rate in small volumes.

3.5.3. Hippocampus

Atrophy rate did not predict time to conversion in hippocampal baseline volumes less than 5500 mm^3, whereas it had significant predictive value at higher volumes. Medium to large volumes were associated with 69% and 95% lower risk of conversion from MCI to AD compared with small volumes. An additional 15% and 50% decrease in the risk of conversion were demonstrated for every 1 percent lower atrophy rate in medium and large volumes.

3.5.4. Entorhinal cortex

Atrophy rate did not predict time to conversion in entorhinal cortex baseline volumes less than 2800 mm^3, whereas it had significant predictive value at large volumes (larger than 4000 mm^3). Medium to large entorhinal cortex volumes were, respectively, associated with 47% and 86% lower risk of conversion from MCI to AD compared with small volumes. An additional 24% decrease in the risk of conversion was demonstrated for 1 percent lower atrophy rate in large entorhinal cortex baseline volumes.

Table 3
Risk of conversion from MCI to AD over time (Cox proportional hazard ratios) in medium and large brain volume categories (small and medium categories in the ventricles) compared with the small brain volume category (large category in the ventricles)

Diagnostic group	Coef.	SE	HR (95% CI)	Z, *p*-value
Whole brain				
Medium whole brain	**−0.96**	**0.21**	**0.39 (0.25−0.58)**	**−4.488, $p < 0.0001$**
Large whole brain	**−1.28**	**0.32**	**0.28 (0.15−0.53)**	**−3.949, $p < 0.0001$**
Atrophy rate[a]	0.08	0.18	1.08 (0.76−1.54)	0.438, $p = 0.66$
Medium whole brain: atrophy rate	**−0.44**	**0.21**	**0.65 (0.43−0.98)**	**−2.072, $p < 0.05$**
Large whole brain: atrophy rate	**−0.56**	**0.34**	**0.57 (0.34−0.96)**	**−2.132, $p < 0.05$**
Ventricles				
Medium ventricles	**−0.65**	**0.32**	**0.52 (0.28−0.97)**	**−2.068, $p < 0.05$**
Small ventricles	**−1.76**	**0.48**	**0.17 (0.07−0.42)**	**−3.664, $p < 0.001$**
Enlargement rate[b]	0.05	0.05	1.05 (0.96−1.15)	1.000, $p = 0.32$
Medium ventricles: atrophy rate	0.04	0.05	1.04 (0.94−1.14)	0.757, $p = 0.45$
Small ventricles: atrophy rate	**0.13**	**0.06**	**1.14 (1.01−1.29)**	**2.065, $p < 0.05$**
Hippocampus				
Medium hippocampus	**−1.16**	**0.28**	**0.31 (0.18−0.54)**	**−4.122, $p < 0.0001$**
Large hippocampus	**−3.09**	**0.50**	**0.05 (0.02−0.12)**	**−6.252, $p < 0.0001$**
Atrophy rate[a]	−0.04	0.05	0.96 (0.86−1.06)	−0.818, $p = 0.41$
Medium hippocampus: atrophy rate	**−0.16**	**0.06**	**0.85 (0.75−0.97)**	**−2.472, $p < 0.05$**
Large hippocampus: atrophy rate	**−0.69**	**0.14**	**0.50 (0.38−0.66)**	**−5.022, $p < 0.0001$**
Entorhinal cortex				
Medium entorhinal	**−0.64**	**0.22**	**0.53 (0.34−0.81)**	**−2.954, $p < 0.01$**
Large entorhinal	**−1.97**	**0.35**	**0.14 (0.07−0.28)**	**−5.600, $p < 0.0001$**
Atrophy rate[a]	−0.05	0.03	0.96 (0.91−1.01)	−1.623, $p = 0.11$
Medium entorhinal: atrophy rate	−0.03	0.04	0.98 (0.90−1.04)	−0.900, $p = 0.37$
Large entorhinal: atrophy rate	**−0.27**	**0.07**	**0.76 (0.67−0.87)**	**−3.941, $p < 0.0001$**

Small category, smaller than one SD below the mean; medium category, one SD below and above the mean; and large category, larger than one SD above the mean.
All measures have been adjusted for age, sex, field strength, and intracranial volume.
Bolded values represents the significance of $p < 0.05$.
Key: AD, Alzheimer's disease; MCI, mild cognitive impairment; Coef, coefficient; SE, standard error; HR, hazard ratio.
[a] Atrophy rate in the small volume category.
[b] Enlargement rate in the large ventricular volume category.

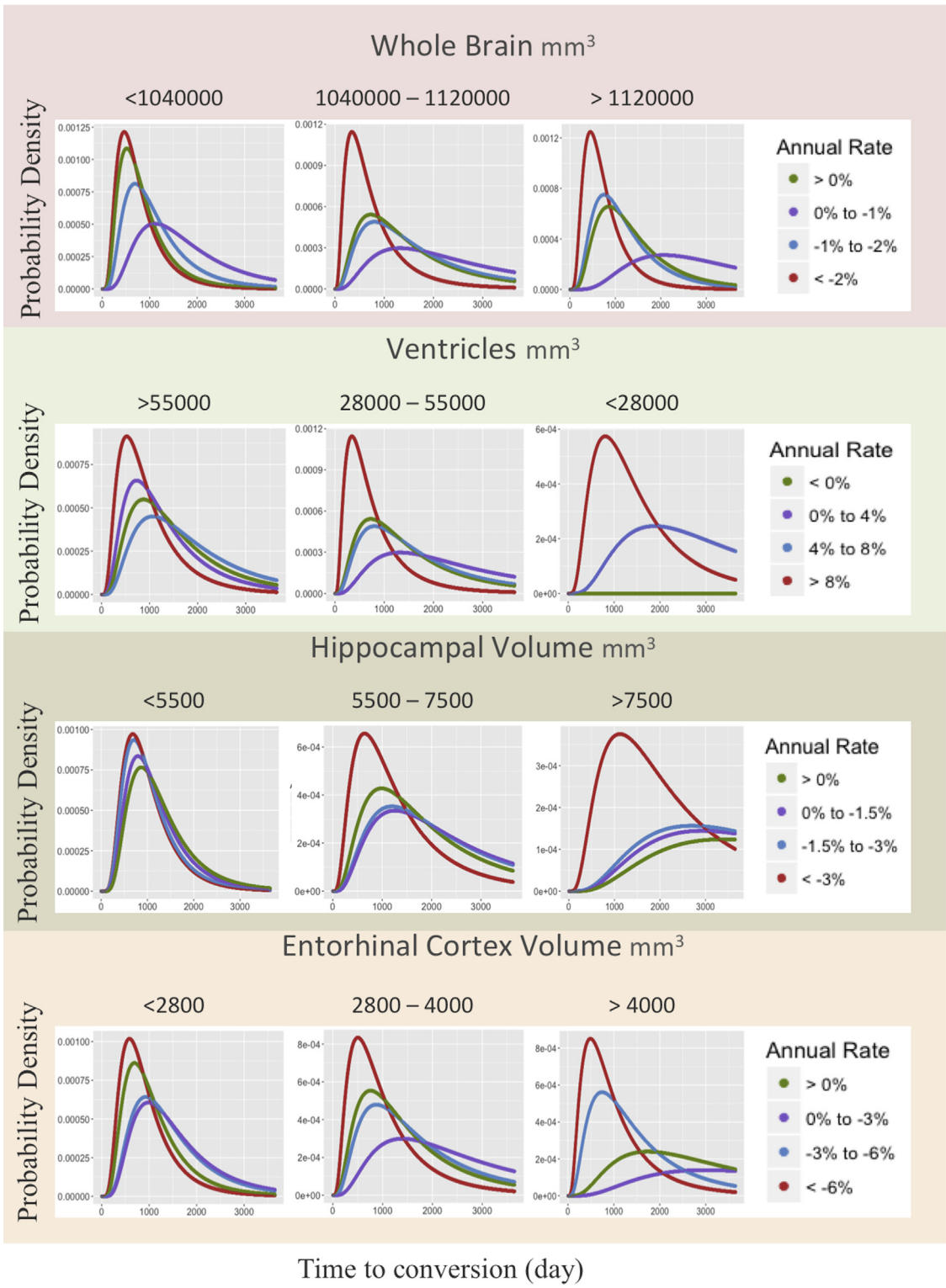

Fig. 1. Distribution of probability of conversion over time: Separate illustration of probability density measured by Cox proportional models in 4 brain areas at 3 baseline categories across stratified respected annual atrophy rate (enlargement rate for the ventricles) within ten years. The figure shows that at hippocampal baseline volumes less than 5500 mm^3, conversions mostly happen within three years regardless of atrophy rate. Similar patterns but relatively less determinant are noticeable at entorhinal cortex volumes lower than 2800 mm^3, at whole brain baseline volumes lower than 1,040,000 mm^3, and at ventricle baseline volumes larger than 55,000 mm^3. By contrast, atrophy rate (enlargement rate for the ventricles) has an impact on probability of conversion over time at medium to large baseline brain volumes (medium to small for the ventricles), especially noticeable for the hippocampus with atrophy rate more than the average.

4. Discussion

This study aimed to investigate of the volume or change in volume over time of different brain regions could predict the time to conversion from MCI to AD. The main finding was that the baseline volumes of the whole brain, ventricles, hippocampus, and entorhinal cortex and their respective atrophy rates (enlargement rate for ventricles) were all significant predictors of earlier conversion. However, the predictive value of these ROIs' atrophy rates was highly dependent on their baseline volume.

Although volume and change in volume over time are predictive across all ROIs, the effect of baseline volume on the predictive value of volume change over time is more distinctive in the hippocampus than other ROIs (Fig. 1). Individuals with hippocampal volumes smaller than 5500 mm^3 mostly convert to AD within three years regardless of atrophy rate. This has an important implication for clinical trials aiming to delay AD conversion by reducing atrophy rate. In these trials, any treatment effects on brain atrophy rate should be interpreted in light of baseline volumes because at small hippocampal volumes, any reduction in atrophy rate is less likely to be associated with delay in disease progression. Indeed, it may be better for clinical trials to exclude individuals with small hippocampal volumes to identify interventions that can really delay the conversion by reducing volume loss. In addition, hippocampal volume can be used as a simple heuristics to identify those at risk of early conversion in clinical practice. However, it is important to note that the baseline brain volumes in this study were normalized for age, sex, field strength, and ICV, and therefore, hippocampal threshold for small volume (i.e., 5500 mm^3) for any individual must be corrected with the provided formula

$$\text{Hippocampal threshold} = \begin{array}{l}\text{Male} \geq 3141 + 74.5 * \text{Age} - 477.5 * \text{field strength} - 0.0014 * \text{ICV} \\ \text{Female} \geq 3438 + 74.5 * \text{Age} - 477.5 * \text{field strength} - 0.0014 * \text{ICV}\end{array}$$

Although we cannot shed light on specific reasons for this hippocampal threshold, we speculate that volumes below this value are indicative of an accumulation of pathology, which makes conversion to AD all but inevitable. Regional accumulation of pathology is associated with concomitant spread of pathology to the adjacent brain areas. At early stages of the disease, neuropathology and brain atrophy is mainly limited to the medial and inferior temporal lobes (including hippocampus and entorhinal cortex) particularly in relation to tauopathy. As the disease progresses, degeneration spreads into more posterior regions of the temporal lobe and starts to spread to the parietal lobe. By the time of conversion to AD, atrophy has become more severe in the areas first affected and has spread further into the frontal lobes (Braak and Braak, 1991; Thal et al., 2002; Whitwell et al., 2007). Therefore, hippocampal volume below a certain threshold is not only indicative of pathology accumulation in this structure but also of spreading neurodegeneration in adjacent regions, which together indicate poorer prognosis.

By contrast, in those with larger ROI volumes, atrophy rate is a predictor of the time to conversion but is dependent on baseline volume. The pattern in larger volumes is also somewhat more distinctive in the hippocampus than other ROIs. Atrophy rate in those with medium to large hippocampal baseline volume (5500 mm^3–7500 mm^3) is determinant of the risk of AD conversion, whereas at volume larger than 7500 mm^3, atrophy rate more than the average, i.e., more than 3%/y, is determinant. This can also be explained by the contribution of previous (reflected in baseline volume) and ensuing (reflecting in atrophy rate) neurodegeneration in prediction of progression. It is likely that at medium baseline volumes, there is a balance between previous and ensuing neurodegeneration; thus both measures are determinant of the time to conversion. While at volume larger than 7500 mm^3, because of low level of previous degeneration, only a large atrophy rate (more than the average of 3%/y) can be determinant of time to AD conversion.

The present results are particularly significant because they provide a guide on how structural imaging measures can assist in predicting conversion to AD as recommended by the National Institute on Aging and the Alzheimer's Association although to date they have been unable to advise on how this should or could be done (Jack et al., 2018). This approach also aligns with our understanding of AD's pathological progression, which recognizes MCI as a clinical stage of the disease continuum, rather than a distinct clinical entity with a higher risk of AD conversion (Albert et al., 2011; Dubois et al., 2016).

It is noteworthy that the selection of the brain ROIs in this study was based on the typical spread of the neurofibrillary tangles and neurodegeneration in the course of the disease. Typically, AD's neurofibrillary tangles aggregation and subsequent neurodegeneration originate in the transentorhinal cortex and spread through the hippocampus to subcortical structures and the lateral temporal, parietal, and frontal association and primary cortices (Braak and Braak, 1991). However, there is some evidence demonstrating the presence of at least 2 atypical subtypes of AD that do not follow the typical pattern, i.e., limbic-predominant AD and hippocampus-sparing AD (Byun et al., 2015; Ferreira et al., 2017; Whitwell et al., 2012). In the limbic-predominant AD, fibrillary tangles and degeneration remain restrictively in medial temporal lobe and cortical areas remain relatively preserved. The hippocampus and entorhinal cortex are severely involved and progression to the final stages of the disease is faster than the other subtypes (Ferreira et al., 2017; Murray et al., 2011). Thus, hippocampal atrophy would be expected to remain predictive of time to conversion, and to be consistent with the present findings. By contrast, in the hippocampus-sparing subtype, the pathology originates in the lateral cortical areas and the medial temporal lobe including the hippocampus remains preserved and hippocampal atrophy is in line with that found in normal aging (Ferreira et al., 2017). Thus, hippocampal atrophy is not expected to be predictive of time to AD conversion. Of relevance to the present findings, the possible presence of this subtype in the sample investigated—it affects approximately 10% of all AD cases in the population—may have negatively impacted the predictive value of the measures investigated, although probably only to a small extent.

To our knowledge, the present study is the first investigation of interaction between brain volume and annual change rate in predicting the time to conversion from MCI to AD. In addition, unlike previous studies, which investigated the prediction of conversion from MCI to AD within follow-ups of 1 to three years (Jack et al., 2005; Liu et al., 2017; McEvoy et al., 2011; Risacher et al., 2009), the follow-up time of the present study was up to ten years. However, these findings need replications in other population before their usefulness in clinical practice can ascertained.

5. Conclusion

These findings are among the first to demonstrate that simple structural imaging measures can make a useful contribution in predicting disease progression from MCI to AD. Importantly, they provide specific guidance on volumetric thresholds in specific brain structures, which can be used to inform clinical assessment. However, while this is an important first step, further investigation in different, more diverse, and larger populations is needed before recommendation for their routine use in clinical trials and clinical practice can be confidently made.

Disclosure

None.

Acknowledgements

Data collection and sharing for this project was funded by the Alzheimer's Disease Neuroimaging Initiative (ADNI; National Institutes of Health Grant U01 AG024904). ADNI is funded by the National Institute on Aging, the National Institute of Biomedical Imaging and Bioengineering, and through generous contributions from the following: Alzheimer's Association; Alzheimer Drug Discovery Foundation; BioClinica, Inc; Biogen Idec Inc; Bristol-Myers Squibb Company; Eisai Inc; Elan Pharmaceuticals, Inc; Eli Lilly and Company; F. Hoffmann-La Roche Ltd and its affiliated company Genentech, Inc; GE Healthcare; Innogenetics, N.V.; IXICO Ltd.; Janssen Alzheimer Immunotherapy Research & Development, LLC.; Johnson & Johnson Pharmaceutical Research & Development LLC.; Medpace, Inc; Merck & Co, Inc; Meso Scale Diagnostics, LLC.; NeuroRx Research; Novartis Pharmaceuticals Corporation; Pfizer Inc; Piramal Imaging; Servier; Synarc Inc; and Takeda Pharmaceutical Company. The Canadian Institutes of Health Research is providing funds to support ADNI clinical sites in Canada. Private sector contributions are facilitated by the Foundation for the National Institutes of Health (www.fnih.org). The grantee organization is the Northern California Institute for Research and Education, and the study is co-ordinated by the Alzheimer's Disease Cooperative Study at the University of California, San Diego. ADNI data are disseminated by the Laboratory for Neuro Imaging at the University of Southern California. This research was partly undertaken on the National Computational Infrastructure (NCI) facility in Canberra, Australia, which is supported by the Australian Commonwealth Government and by an Australian Government Research Training Program (RTP) Scholarship.

This research did not receive any specific grant from funding agencies in the public, commercial, or not-for-profit sectors.

Appendix A. Supplementary data

Supplementary data to this article can be found online at https://doi.org/10.1016/j.neurobiolaging.2019.08.033.

References

Albert, M.S., DeKosky, S.T., Dickson, D., Dubois, B., Feldman, H.H., Fox, N.C., Gamst, A., Holtzman, D.M., Jagust, W.J., Petersen, R.C., Snyder, P.J., Carrillo, M.C., Thies, B., Phelps, C.H., 2011. The diagnosis of mild cognitive impairment due to Alzheimer's disease: recommendations from the National Institute on Aging-Alzheimer's Association workgroups on diagnostic guidelines for Alzheimer's disease. Alzheimers Dement. 7, 270–279.

Braak, H., Braak, E., 1991. Neuropathological stageing of Alzheimer-related changes. Acta Neuropathol. 82, 239–259.

Braak, H., Braak, E., 1997. Frequency of stages of Alzheimer-related lesions in different age categories. Neurobiol. Aging 18, 351–357.

Byun, M.S., Kim, S.E., Park, J., Yi, D., Choe, Y.M., Sohn, B.K., Choi, H.J., Baek, H., Han, J.Y., Woo, J.I., Lee, D.Y., Alzheimer's Disease Neuroimaging, I, 2015. Heterogeneity of regional brain atrophy patterns associated with distinct progression rates in Alzheimer's disease. PLoS One 10, e0142756.

Douaud, G.l., Refsum, H., de Jager, C.A., Jacoby, R., Nichols, T.E., Smith, S.M., Smith, A.D., 2013. Preventing Alzheimer's disease-related gray matter atrophy by B-vitamin treatment. Proc. Natl. Acad. Sci. U. S. A. 110, 9523–9528.

Dubois, B., Chupin, M., Hampel, H., Lista, S., Cavedo, E., Croisile, B., Louis Tisserand, G., Touchon, J., Bonafe, A., Ousset, P.J., Ait Ameur, A., Rouaud, O., Ricolfi, F., Vighetto, A., Pasquier, F., Delmaire, C., Ceccaldi, M., Girard, N., Dufouil, C., Lehericy, S., Tonelli, I., Duveau, F., Colliot, O., Garnero, L., Sarazin, M., Dormont, D., Hippocampus Study, G., Hippocampus Study, G., 2015. Donepezil decreases annual rate of hippocampal atrophy in suspected prodromal Alzheimer's disease. Alzheimers Dement. 11, 1041–1049.

Dubois, B., Hampel, H., Feldman, H.H., Scheltens, P., Aisen, P., Andrieu, S., Bakardjian, H., Benali, H., Bertram, L., Blennow, K., Broich, K., Cavedo, E., Crutch, S., Dartigues, J.F., Duyckaerts, C., Epelbaum, S., Frisoni, G.B., Gauthier, S., Genthon, R., Gouw, A.A., Habert, M.O., Holtzman, D.M., Kivipelto, M., Lista, S., Molinuevo, J.L., O'Bryant, S.E., Rabinovici, G.D., Rowe, C., Salloway, S., Schneider, L.S., Sperling, R., Teichmann, M., Carrillo, M.C., Cummings, J., Jack Jr., C.R., Proceedings of the Meeting of the International Working, G., the American Alzheimer's Association on "The Preclinical State of, A.D., July, Washington Dc, U.S.A, 2016. Preclinical Alzheimer's disease: definition, natural history, and diagnostic criteria. Alzheimer's & dementia. J. Alzheimers Assoc. 12, 292–323.

Falahati, F., Ferreira, D., Muehlboeck, J.S., Eriksdotter, M., Simmons, A., Wahlund, L.O., Westman, E., 2017. Monitoring disease progression in mild cognitive impairment: associations between atrophy patterns, cognition, APOE and amyloid. Neuroimage Clin. 16, 418–428.

Ferreira, D., Verhagen, C., Hernandez-Cabrera, J.A., Cavallin, L., Guo, C.J., Ekman, U., Muehlboeck, J.S., Simmons, A., Barroso, J., Wahlund, L.O., Westman, E., 2017. Distinct subtypes of Alzheimer's disease based on patterns of brain atrophy: longitudinal trajectories and clinical applications. Sci. Rep. 7, 46263.

Fjell, A.M., Westlye, L.T., Grydeland, H., Amlien, I., Espeseth, T., Reinvang, I., Raz, N., Dale, A.M., Walhovd, K.B., 2014. Accelerating cortical thinning: unique to dementia or universal in aging? Cereb. Cortex 24, 919–934.

Gavidia-Bovadilla, G., Kanaan-Izquierdo, S., Mataro-Serrat, M., Perera-Lluna, A., Alzheimer's Disease Neuroimaging, I, 2017. Early prediction of Alzheimer's disease using null longitudinal model-based classifiers. PLoS One 12, e0168011.

Jack Jr., C.R., Bennett, D.A., Blennow, K., Carrillo, M.C., Dunn, B., Haeberlein, S.B., Holtzman, D.M., Jagust, W., Jessen, F., Karlawish, J., Liu, E., Molinuevo, J.L., Montine, T., Phelps, C., Rankin, K.P., Rowe, C.C., Scheltens, P., Siemers, E., Snyder, H.M., Sperling, R., Contributors, 2018. NIA-AA Research Framework: toward a biological definition of Alzheimer's disease. Alzheimers Dement. 14, 535–562.

Jack Jr., C.R., Bernstein, M.A., Fox, N.C., Thompson, P., Alexander, G., Harvey, D., Borowski, B., Britson, P.J., J, L.W., Ward, C., Dale, A.M., Felmlee, J.P., Gunter, J.L., Hill, D.L., Killiany, R., Schuff, N., Fox-Bosetti, S., Lin, C., Studholme, C., DeCarli, C.S., Krueger, G., Ward, H.A., Metzger, G.J., Scott, K.T., Mallozzi, R., Blezek, D., Levy, J., Debbins, J.P., Fleisher, A.S., Albert, M., Green, R., Bartzokis, G., Glover, G., Mugler, J., Weiner, M.W., 2008. The Alzheimer's disease neuroimaging initiative (ADNI): MRI methods. J. Magn. Reson. Imaging 27, 685–691.

Jack Jr., C.R., Shiung, M.M., Weigand, S.D., O'Brien, P.C., Gunter, J.L., Boeve, B.F., Knopman, D.S., Smith, G.E., Ivnik, R.J., Tangalos, E.G., Petersen, R.C., 2005. Brain atrophy rates predict subsequent clinical conversion in normal elderly and amnestic MCI. Neurology 65, 1227–1231.

Kile, S., Au, W., Parise, C., Rose, K., Donnel, T., Hankins, A., Chan, M., Ghassemi, A., 2017. IVIG treatment of mild cognitive impairment due to Alzheimer's disease: a randomised double-blinded exploratory study of the effect on brain atrophy, cognition and conversion to dementia. J. Neurol. Neurosurg. Psychiatry 88, 106–112.

Kobe, T., Witte, A.V., Schnelle, A., Lesemann, A., Fabian, S., Tesky, V.A., Pantel, J., Floel, A., 2016. Combined omega-3 fatty acids, aerobic exercise and cognitive stimulation prevents decline in gray matter volume of the frontal, parietal and cingulate cortex in patients with mild cognitive impairment. Neuroimage 131, 226–238.

Li, Y., Wang, Y., Wu, G., Shi, F., Zhou, L., Lin, W., Shen, D., 2012. Discriminant analysis of longitudinal cortical thickness changes in Alzheimer's disease using dynamic and network features. Neurobiol. Aging 33, 427.e15–427.e30.

Liu, K., Chen, K., Yao, L., Guo, X., 2017. Prediction of mild cognitive impairment conversion using a combination of independent component analysis and the Cox model. Front Hum. Neurosci. 11, 33.

McEvoy, L.K., Holland, D., Donald, J., Hagler, J., Fennema-Notestine, C., Brewer, J.B., Dale, A.M., 2011. Mild cognitive impairment: baseline and longitudinal structural MR imaging measures improve predictive Prognosis1. Radiology 259, 834–843.

Murray, M.E., Graff-Radford, N.R., Ross, O.A., Petersen, R.C., Duara, R., Dickson, D.W., 2011. Neuropathologically defined subtypes of Alzheimer's disease with distinct clinical characteristics: a retrospective study. Lancet Neurol. 10, 785–796.

Petersen, R.C., Aisen, P.S., Beckett, L.A., Donohue, M.C., Gamst, A.C., Harvey, D.J., Jack, C.R., Jagust, W.J., Shaw, L.M., Toga, A.W., Trojanowski, J.Q., Weiner, M.W., 2010. Alzheimer's disease neuroimaging initiative (ADNI) clinical characterization. Neurology 74, 201–209.

Pintzka, C.W., Hansen, T.I., Evensmoen, H.R., Haberg, A.K., 2015. Marked effects of intracranial volume correction methods on sex differences in neuroanatomical structures: a HUNT MRI study. Front Neurosci. 9, 238.

Prins, N.D., van der Flier, W.A., Knol, D.L., Fox, N.C., Brashear, H., Nye, J.S., Barkhof, F., Scheltens, P., 2014. The effect of galantamine on brain atrophy rate in subjects with mild cognitive impairment is modified by apolipoprotein E genotype: post-hoc analysis of data from a randomized controlled trial. Alzheimers Res. Ther. 6, 47.

Risacher, S.L., Saykin, A.J., West, J.D., Shen, L., Firpi, H.A., McDonald, B.C., Alzheimer's Disease Neuroimaging, I, 2009. Baseline MRI predictors of conversion from MCI to probable AD in the ADNI cohort. Curr. Alzheimer Res. 6, 347–361.

Risacher, S.L., Shen, L., West, J.D., Kim, S., McDonald, B.C., Beckett, L.A., Harvey, D.J., Jack Jr., C.R., Weiner, M.W., Saykin, A.J., Alzheimer's Disease Neuroimaging, I, 2010. Longitudinal MRI atrophy biomarkers: relationship to conversion in the ADNI cohort. Neurobiol. Aging 31, 1401–1418.

Tabatabaei-Jafari, H., Shaw, M.E., Cherbuin, N., 2015. Cerebral atrophy in mild cognitive impairment: a systematic review with meta-analysis. Alzheimers Dement. 1, 487–504.

Tabatabaei-Jafari, H., Shaw, M.E., Walsh, E., Cherbuin, N., Alzheimer's Disease Neuroimaging, I, 2019. Cognitive/functional measures predict Alzheimer's disease, dependent on hippocampal volume. J. Gerontol. B Psychol. Sci. Soc. Sci.

Teipel, S.J., Kurth, J., Krause, B., Grothe, M.J., Alzheimer's Disease Neuroimaging, I, 2015. The relative importance of imaging markers for the prediction of Alzheimer's disease dementia in mild cognitive impairment - beyond classical regression. Neuroimage Clin. 8, 583–593.

Thal, D.R., Rub, U., Orantes, M., Braak, H., 2002. Phases of A beta-deposition in the human brain and its relevance for the development of AD. Neurology 58, 1791–1800.

Thung, K.H., Yap, P.T., Adeli, E., Lee, S.W., Shen, D., Alzheimer's Disease Neuroimaging, I, 2018. Conversion and time-to-conversion predictions of mild cognitive impairment using low-rank affinity pursuit denoising and matrix completion. Med. Image Anal. 45, 68–82.

Whitwell, J.L., Dickson, D.W., Murray, M.E., Weigand, S.D., Tosakulwong, N., Senjem, M.L., Knopman, D.S., Boeve, B.F., Parisi, J.E., Petersen, R.C., Jack, C.R., Josephs, K.A., 2012. Neuroimaging correlates of pathologically defined subtypes of Alzheimer's disease: a case-control study. Lancet Neurol. 11, 868–877.

Whitwell, J.L., Przybelski, S.A., Weigand, S.D., Knopman, D.S., Boeve, B.F., Petersen, R.C., Jack Jr., C.R., 2007. 3D maps from multiple MRI illustrate changing atrophy patterns as subjects progress from mild cognitive impairment to Alzheimer's disease. Brain. 130 (Pt 7), 1777–1786.

Zhang, Y.P., Miao, R., Li, Q., Wu, T., Ma, F., 2017. Effects of DHA supplementation on hippocampal volume and cognitive function in older adults with mild cognitive impairment: a 12-month randomized, double-blind, placebo-controlled trial. J. Alzheimers Dis. 55, 497–507.